5. Template–Based Synthesis of Nanorod or Nanowire Arrays

Huamei (Mary) Shang, Guozhong Cao

This chapter introduces the fundamentals of and various technical approaches developed for template–based synthesis of nanorod arrays. After a brief introduction to various concepts associated with the growth of nanorods, nanowires and nanobelts, the chapter focuses mainly on the most widely used and well established techniques for the template–based growth of nanorod arrays: electrochemical deposition, electrophoretic deposition, template filling via capillary force and centrifugation, and chemical conversion. In each section, the relevant fundamentals are first introduced, and then examples are given to illustrate the specific details of each technique.

Part A | 5

Syntheses, characterizations and applications of nanowires, nanorods, nanotubes and nanobelts (also often referred to as one-dimensional nanostructures) are significant areas of current endeavor in nanotechnology. Many techniques have been developed in these areas, and our understanding of the field has been significantly enhanced [5.1–5]. The field is still evolving rapidly with new synthesis methods and new nanowires or nanorods reported in the literature. Evaporation–condensation growth has been successfully applied to the synthesis of various oxide nanowires and nanorods. Similarly, the dissolution–condensation method has been widely used for the synthesis of various metallic nanowires from solutions. The vapor–liquid–solid (VLS) growth method is a highly versatile approach; various elementary and compound semiconductor nanowires have been synthesized using this method [5.6]. Template-based growth of nanowires or nanorods is an even more versatile method for various materials. Substrate ledge or step-induced growth of nanowires or nanorods has also been investigated intensively [5.7]. Except for VLS and template-based growth, most of the above-mentioned methods result in randomly oriented nanowires or nanorods (commonly in the form of powder). The VLS method provides the ability to grow well oriented nanorods or nanowires directly attached to substrates, and is therefore often advantageous for characterization and applications; however, catalysts are required to form a liquid capsule at the advancing surface during growth at elevated temperatures. In addition, the possible incorporation of catalyst into nanowires and the difficulty removing such capsules from the tips of nanowires or nanorods are two disadvantages of this technique. Template-based growth often suffers from the polycrystalline nature of the resultant nanowires and nanorods, in addition to the dif-

ficulties involved in finding appropriate templates with pore channels of a desired diameter, length and surface chemistry and in removing the template completely without compromising the integrity of grown nanowires or nanorods. The discussion in this chapter will focus on nanorod and nanowire arrays, although nanotube arrays are mentioned briefly in conjunction with nanorod and nanowire fabrication. In addition, the terms of *nanorod* and *nanowire* are used interchangeably without special distinction in this chapter; this is commonplace in the literature.

In comparison with nanostructured materials in other forms, nanorod arrays offer several advantages for studying properties and for practical applications. Significant progress has been made in studies of the physical properties of individual nanowires and nanorods performed by directly measuring the proper-

ties of individual nanostructures. However, such studies generally require a lot of experimental preparation. For example, for electrical conductivity measurements, patterned electrodes are first created on a substrate, and then nanowires or nanorods are dispersed in an appropriate solvent or solution. This nanowire colloidal dispersion is then cast on the substrate containing pattern electrodes. Measurements are carried out after identifying individual nanowires or nanorods bridging two electrodes. The options for manipulating nanowires or nanorods are limited, and it is difficult to improve the contact between the sample and the electrodes to ensure the desired ohmic contact. For practical applications, the output or signal generated by single nanowire- or nanorod-based devices is small, and the signal-to-noise ratio is small, which means that highly sensitive instrumentation is required to accommodate such devices.

5.1 Template–Based Approach

The template approach to preparing free-standing, non-oriented and oriented nanowires and nanorods has been investigated extensively. The most commonly used and commercially available templates are anodized alumina membrane (AAM) [5.8] and radiation track-etched polycarbonate (PC) membranes [5.9]. Other membranes have also been used, such as nanochannel array on glass [5.10], radiation track-etched mica [5.11], mesoporous materials [5.12], porous silicon obtained via electrochemical etching of silicon wafer [5.13], zeolites [5.14] and carbon nanotubes [5.15,16]. Biotemplates have also been explored for the growth of nanowires [5.17] and nanotubes [5.18], such as Cu [5.19], Ni [5.17], Co [5.17], and Au [5.20] nanowires. Commonly used alumina membranes with uniform and parallel pores are produced by the anodic oxidation of aluminium sheet in solutions of sulfuric, oxalic, or phosphoric acids [5.8, 21]. The pores can be arranged in a regular hexagonal array, and densities as high as 10^{11} pores/cm^2 can be achieved [5.22]. Pore size ranging from 10 nm to 100 μm can be achieved [5.22, 23]. PC membranes are made by bombarding a nonporous polycarbonate sheet, typically 6 to 20 μm in thickness, with nuclear fission fragments to create damage tracks, and then chemically etching these tracks into pores [5.9]. In these radiation track-etched membranes, the pores are of uniform size (as small as 10 nm), but they are randomly distributed. Pore densities can be as high as 10^9 pores/cm^2.

In addition to the desired pore or channel size, morphology, size distribution and density of pores, template materials must meet certain requirements. First, the template materials must be compatible with the processing conditions. For example, an electrical insulator is required when a template is used in electrochemical deposition. Except in the case of template-directed synthesis, the template materials should be chemically and thermally inert during synthesis and the following processing steps. Secondly, the material or solution being deposited must wet the internal pore walls. Thirdly, for the synthesis of nanorods or nanowires, the deposition should start from the bottom or from one end of the template channel and proceed from one side to the other. However, for the growth of nanotubules, deposition should start from the pore wall and proceed inwardly. Inward growth may result in pore blockage, so this should be avoided during the growth of *solid* nanorods or nanowires. Kinetically, the correct amount of surface relaxation permits maximal packing density, so a diffusion-limited process is preferred. Other considerations include the ease of release of the nanowires or nanorods from the templates and the ease of handling during the experiments.

AAM and PC membranes are most commonly used for the synthesis of nanorod or nanowire arrays. Both templates are very convenient for the growth of nanorods by various growth mechanisms, but each type of template also has its disadvantages. The advantages

of using PC as the template are its easy handling and easy removal by means of pyrolysis at elevated temperatures, but the flexibility of PC is more prone to distortion during the heating process, and removal of the template occurs before complete densification of the nanorods. These factors result in broken and deformed nanorods. The advantage of using AAM as the template is its rigidity and resistance to high temperatures, which allows the nanorods to densify completely before removal. This results in fairly free-standing and unidirectionally-aligned nanorod arrays with a larger surface area than for PC. The problem with AAM is the complete removal of the template after nanorod growth, which is yet to be achieved when using wet chemical etching.

5.2 Electrochemical Deposition

Electrochemical deposition, also known as electrodeposition, involves the oriented diffusion of charged reactive species through a solution when an external electric field is applied, and the reduction of the charged growth species at the growth or deposition surface (which also serves as an electrode). In industry, electrochemical deposition is widely used when coating metals in a process known as electroplating [5.25]. In general, this method is only applicable to electrically conductive materials such as metals, alloys, semiconductors, and electrically conductive polymers. After the initial deposition, the electrode is separated from the depositing solution by the deposit and so the deposit must conduct in order to allow the deposition process to continue. When the deposition is confined to the pores of template membranes, nanocomposites are produced. If the template membrane is removed, nanorod or nanowire arrays are prepared.

When a solid is immersed in a polar solvent or an electrolyte solution, surface charge will develop. The electrode potential is described by the Nernst equation

$$E = E_0 + \frac{RT}{n_i F} \ln (a_i) \ , \tag{5.1}$$

where E_0 is the standard electrode potential (or the potential difference between the electrode and the solution) when the activity a_i of the ions is unity, F is Faraday's constant, R is the gas constant, and T is the temperature. When the electrode potential is higher than
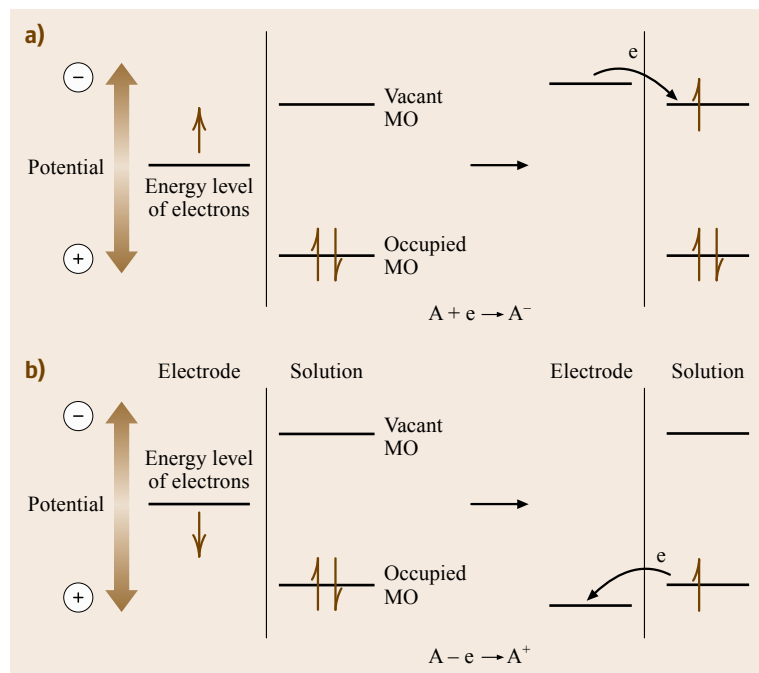
Fig. 5.1a,b Representation of the reduction **(a)** and oxidation **(b)** of a species A in solution. The molecular orbitals (MO) shown for species A are the highest occupied MO and the lowest vacant MO. These approximately correspond to the E_0's of the A/A$^-$ and A$^+$/A couples, respectively (after [5.24])

the energy level of a vacant molecular orbital in the electrolyte, electrons will transfer from the electrode to the solution and the electrolyte will be reduced, as shown in Fig. 5.1a [5.24]. On the other hand, if the electrode potential is lower than the energy level of an occupied molecular orbital in the electrolyte, the electrons will transfer from the electrolyte to the electrode, resulting in electrolyte oxidation, as illustrated in Fig. 5.1b [5.24]. These reactions stop when equilibrium is achieved.

When an external electric field is applied between two dissimilar electrodes, charged species flow from one electrode to the other, and electrochemical reactions occur at both electrodes. This process, called electrolysis, converts electrical energy to chemical potential.
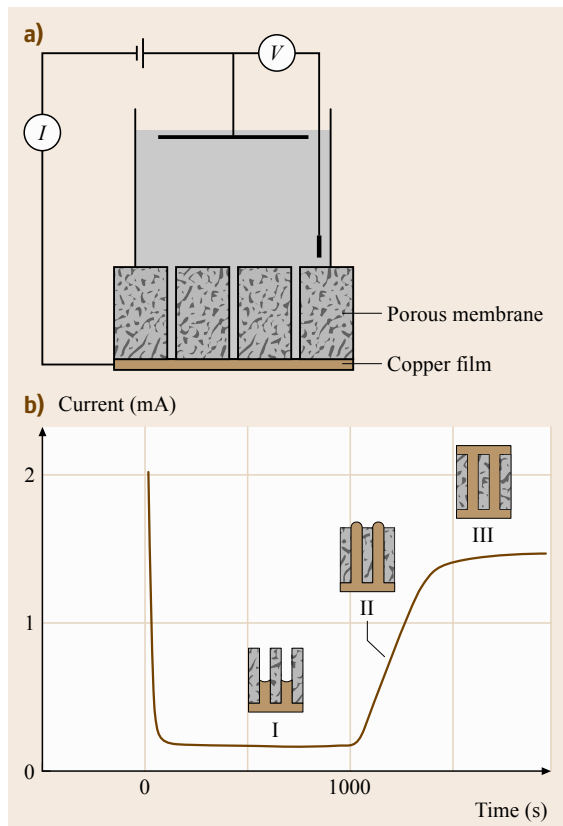

Fig. 5.2a,b Common experimental setup for the template-based growth of nanowires using electrochemical deposition. (**a**) Schematic illustration of the arrangement of the electrodes for nanowire deposition. (**b**) Current–time curve for electrodeposition of Ni into a polycarbonate membrane with 60 nm diameter pores at −1.0 V. *Insets* depict the different stages of the electrodeposition (after [5.26])

The system used to perform electrolysis is called an electrolytic cell. In this cell, the electrode connected to the positive side of the power supply, termed the *anode*, is where an oxidation reaction takes place, whereas the electrode connected to the negative side of the power supply, the *cathode*, is where a reduction reaction proceeds, accompanied by deposition. Therefore, electrolytic deposition is also called cathode deposition, but it is most commonly referred to as electrochemical deposition or electrodeposition.

5.2.1 Metals

The growth of nanowires of conductive materials in an electric field is a self-propagating process [5.27]. Once the small rods form, the electric field and the density of current lines between the tips of nanowires and the opposing electrode are greater than that between two electrodes, due to the shorter distances between the nanowires and the electrodes. This ensures that the species being deposited is constantly attracted preferentially to the nanowire tips, resulting in continued growth. To better control the morphology and size, templates containing channels in the desired shape are used to guide the growth of nanowires. Figure 5.2 illustrates a common setup used for the template-based growth of nanowires [5.26]. The template is attached to the cathode, which is brought into contact with the deposition solution. The anode is placed in the deposition solution, parallel to the cathode. When an electric field is applied, cations diffuse through the channels and deposit on the cathode, resulting in the growth of nanowires inside the template. This figure also shows the current density at different stages of deposition when a constant electric field is applied. The current does not change significantly until the pores are completely filled, at which point the current increases rapidly due to improved contact with the electrolyte solution. The current saturates once the template surface is completely covered. This approach has yielded nanowires made from different metals, including Ni, Co, Cu and Au, with nominal pore diameters of between 10 and 200 nm. The nanowires were found to be true replicas of the pores [5.28]. *Possin* [5.11] prepared various metallic nanowires using radiation track-etched mica. Likewise, *Williams* and *Giordano* [5.29] produced silver nanowires with diameters of less than 10 nm. *Whitney* et al. [5.26] fabricated arrays of nickel and cobalt nanowires, also using PC templates. Single crystal bismuth nanowires have been grown in AAM using pulsed electrodeposition and Fig. 5.3 shows SEM and TEM images
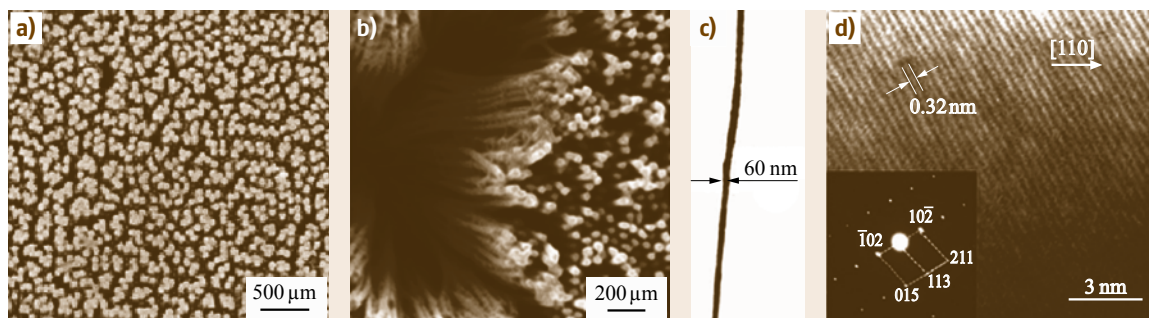
Fig. 5.3a−d SEM images of Bi nanowire arrays: **(a)** top view, **(b)** tilt view. **(c)** TEM image of a typical Bi single nanowire. **(d)** HRTEM image of a typical Bi single nanowire. The *inset* is the corresponding ED pattern (after [5.30])

of the bismuth nanowires [5.30]. Single crystal copper and lead nanowires were prepared by DC electrodeposition and pulse electrodeposition, respectively [5.31, 32]. The growth of single crystal lead nanowires required a greater departure from equilibrium conditions (greater overpotential) compared to the conditions required for polycrystalline ones.

Hollow metal tubules can also be prepared [5.33, 34]. In this case the pore walls of the template are chemically modified by anchoring organic silane molecules so that the metal will preferentially deposit onto the pore walls instead of the bottom electrode. For example, the porous surface of an anodic alumina template was first covered with cyanosilanes; subsequent electrochemical deposition resulted in the growth of gold tubules [5.35]. An electroless electrolysis process has also been investigated for the growth of nanowires and nanorods [5.16, 33, 36]. Electroless deposition is actually a chemical deposition process and it involves the use of a chemical agent to coat a material onto the template surface [5.37]. The main differences between electrochemical deposition and electroless deposition are that the deposition begins at the bottom electrode and the deposited materials must be electrically conductive in the former. The electroless method does not require the deposited materials to be electrically conductive, and the deposition starts from the pore wall and proceeds inwardly. Therefore, in general, electrochemical deposition results in the formation of *solid* nanorods or nanowires of conductive materials, whereas electroless deposition often results in hollow fibrils or nanotubules. For electrochemical deposition, the length of nanowires or nanorods can be controlled by the deposition time, whereas in electroless deposition the length of the nanotubules is solely dependent on the length of the deposition channels or pores. Variation of deposition time would result in a different wall

thickness of nanotubules. An increase in deposition time leads to a thick wall, but sometimes the hollow tubule morphology persists even after prolonged deposition.

Although many research groups have reported on the growth of uniformly sized nanorods and nanowires on PC template membranes, *Schönenberger* et al. [5.38] reported that the channels of carbonate membranes were not always uniform in diameter. They grew Ni, Co, Cu, and Au nanowires using polycarbonate membranes with nominal pore diameters of between 10 and 200 nm by an electrolysis method. From both a potentiostatic study of the growth process and a SEM analysis of nanowire morphology, they concluded that the pores were generally not cylindrical with a constant cross section, but instead were rather cigarlike. For pores with a nominal diameter of 80 nm, the middle section of the pores was wider by up to a factor of 3.

5.2.2 Semiconductors

Semiconductor nanowire and nanorod arrays have been synthesized using AAM templates, such as CdSe and CdTe [5.39]. The synthesis of nanowire arrays of bismuth telluride (Bi_2Te_3) provide a good example of the synthesis of compound nanowire arrays by electrochemical deposition. Bi_2Te_3 is of special interest as a thermoelectric material and Bi_2Te_3 nanowire arrays are believed to offer high figures of merit for thermal-electrical energy conversion [5.40, 41]. Both polycrystalline and single crystal Bi_2Te_3 nanowire arrays have been grown by electrochemical deposition inside anodic alumina membranes [5.42, 43]. *Sander* and coworkers [5.42] fabricated Bi_2Te_3 nanowire arrays with diameters as small as ≈ 25 nm from a solution of 0.075 M Bi and 0.1 M Te in 1 M HNO_3 by electrochemical deposition at -0.46 V versus a Hg/Hg_2SO_4
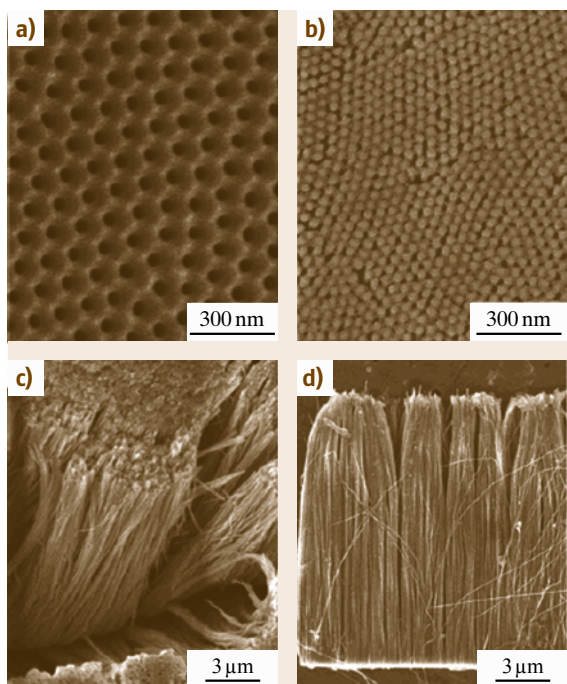
Fig. 5.4a–d SEM photographs of AAM template and Bi_2Te_3 nanowire arrays. **(a)** A typical SEM photograph of AAM. **(b)** Surface view of Bi_2Te_3 nanowire array (eroding time: 5 min). **(c)** Surface view of Bi_2Te_3 nanowire array (eroding time: 15 min). **(d)** Cross-sectional view of Bi_2Te_3 nanowire array (eroding time: 15 min) (after [5.43])

reference electrode. The resultant Bi_2Te_3 nanowire arrays are polycrystalline in nature, and subsequent melting-recrystallization failed to produce single crystal Bi_2Te_3 nanowires. More recently, single crystal Bi_2Te_3 nanowire arrays have been grown from a solution consisted of 0.035 M $Bi(NO_3)_3 \cdot 5H_2O$ and 0.05 M $HTeO_2^+$; the latter was prepared by dissolving Te powder in 5 M HNO_3 by electrochemical deposition. Figure 5.4a shows a typical SEM image of AAM. Both Fig. 5.4b and Fig. 5.4c are surface view of Bi_2Te_3 nanowire array with different eroding time, Fig. 5.4b is 5 min and Fig. 5.4c is 15 min. Figure 5.4d is cross-sectional view of Bi_2Te_3 nanowire array. Figure 5.5 shows TEM image of a cross section of a Bi_2Te_3 nanowire array and an XRD spectrum showing its crystal orientation, respectively. High-resolution TEM and electron diffraction, together with XRD, revealed that [110] is the preferred growth direction of Bi_2Te_3 nanowires. Single crystal nanowire or nanorod arrays can also be made by carefully controlling the initial deposition [5.44]. Simi-

larly, large area Sb_2Te_3 nanowire arrays have also been successfully grown by template-based electrochemical deposition, but the nanowires grown are polycrystalline and show no clear preferred growth direction [5.45].

5.2.3 Conductive Polymers

Electrochemical deposition has also been explored for the synthesis of conductive polymer nanowire and nanorod arrays [5.46]. Conductive polymers have great potential for plastic electronics and sensor applications [5.47, 48]. For example, *Schönenberger* et al. [5.38] have made conductive polyporrole nanowires in PC membranes. Nanotubes are commonly observed for polymer materials, as shown in Fig. 5.6 [5.49], in contrast to *solid* metal nanorods or nanowires. It seems that deposition or solidification of polymers inside template pores starts at the surface and proceeds inwardly. *Martin* [5.50] proposed that this phenomenon was caused by the electrostatic attraction between the growing polycationic polymer and the anionic sites along the pore walls of the polycarbonate membrane. In addition, although the monomers are soluble, the polymerized form is insoluble. Hence there is a solvophobic component leading to deposition at the surface of the pores [5.51, 52]. In the final stage, the diffusion of monomers through the inner pores becomes retarded and monomers inside the pores are quickly depleted. The deposition of polymer inside the inner pores stops.

Liang et al. [5.53] reported a direct electrochemical synthesis of oriented nanowires of polyaniline (PANI) – a conducting polymer with a conjugated backbone due to phenyl and amine groups – from solutions using no templates. The experimental design is based on the idea that, in theory, the rate of electropolymerization (or nanowire growth) is related to the current density. Therefore, it is possible to control the nucleation and the polymerization rate simply by adjusting the current density. The synthesis involves electropolymerization of aniline ($C_6H_5NH_2$) and in situ electrodeposition, resulting in nanowire growth.

5.2.4 Oxides

Similar to metals, semiconductors and conductive polymers, some oxide nanorod arrays can be grown directly from solution by electrochemical deposition. For example, V_2O_5 nanorod arrays have been grown on ITO substrate from $VOSO_4$ aqueous solution with VO^{2+} as the growth species [5.54]. At the interface between the
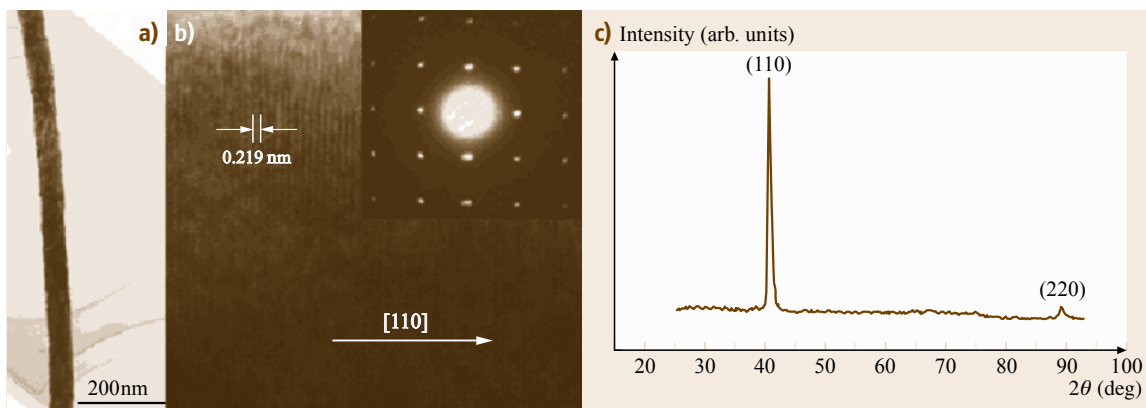
Fig. 5.5a–c TEM images and XRD pattern of a single Bi_2Te_3 nanowire. **(a)** TEM image and **(b)** HRTEM image of the same nanowire. The *inset* is the corresponding ED pattern. **(c)** XRD pattern of Bi_2Te_3 nanowire array (electrodeposition time: 5 min) (after [5.43])
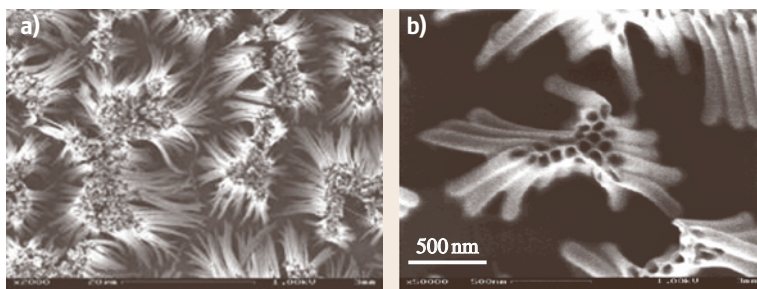
Fig. 5.6a,b SEM images of polymer nanotubes (after [5.49])

electrode (and therefore the subsequent growth surface) and the electrolyte solution, the ionic cluster (VO^{2+}) is oxidized and solid V_2O_5 is deposited through the following reaction

$$2VO^{2+} + 3H_2O \rightarrow V_2O_5 + 6H^+ + 2e^- . \qquad (5.2)$$
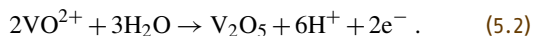
A reduction reaction takes place at the counter electrode

$$2H^+ + 2e^- \rightarrow H_2(g) . \qquad (5.3)$$

It is obvious that the pH and the concentration of VO^{2+} clusters in the vicinity of the growth surface shift away from that in the bulk solution; both the pH and the VO^{2+} concentration decrease.

ZnO nanowire arrays were fabricated by a one-step electrochemical deposition technique based on an ordered nanoporous alumina membrane [5.55]. The ZnO nanowire array is uniformly assembled into the nanochannels of an anodic alumina membrane and consists of single crystal particles.

5.3 Electrophoretic Deposition

The electrophoretic deposition technique has been widely explored, particularly for the deposition of ceramic and organoceramic materials onto a cathode from colloidal dispersions [5.56–58]. Electrophoretic deposition differs from electrochemical deposition in several aspects. First, the material deposited in the electrophoretic deposition method does not need to be electrically conductive. Second, nanosized particles in

colloidal dispersions are typically stabilized by electrostatic or electrosteric mechanisms. As discussed in the previous section, when dispersed in a polar solvent or an electrolyte solution, the surface of a nanoparticle develops an electrical charge via one or more of the following mechanisms: (1) preferential dissolution, (2) deposition of charges or charged species, (3) preferential reduction or oxidation, and (4) physical adsorption of charged
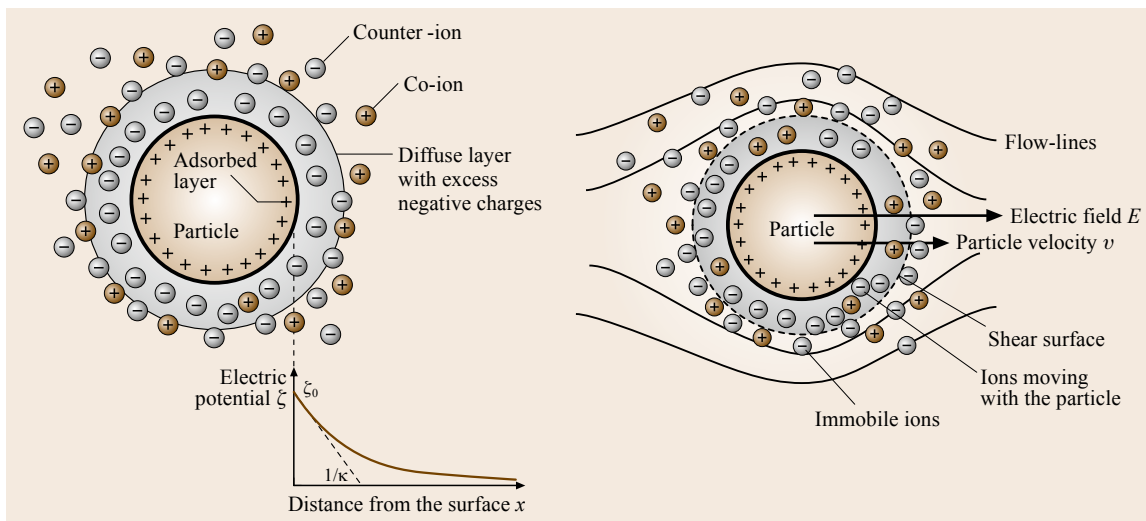
Fig. 5.7 Schematic illustrating electrical double layer structure and the electric potential near the solid surface with both the Stern and Gouy layers indicated. Surface charge is assumed to be positive (after [5.59])

species such as polymers. A combination of electrostatic forces, Brownian motion and osmotic forces results in the formation of a *double layer structure*, schematically illustrated in Fig. 5.7. The figure depicts a positively charged particle surface, the concentration profiles of negative ions (counterions) and positive ions (surface charge-determining ions), and the electric potential profile. The concentration of counterions gradually decreases with distance from the particle surface, whereas that of charge-determining ions increases. As a result, the electric potential decreases with distance. Near the particle surface, the electric potential decreases linearly, in the region known as the Stern layer. Outside of the Stern layer, the decrease follows an exponential relationship. The region between the Stern layer and the point where the electric potential equals zero is called

the diffusion layer. Taken together, the Stern layer and diffusion layer is known as the double layer structure in the classical theory of electrostatic stabilization.
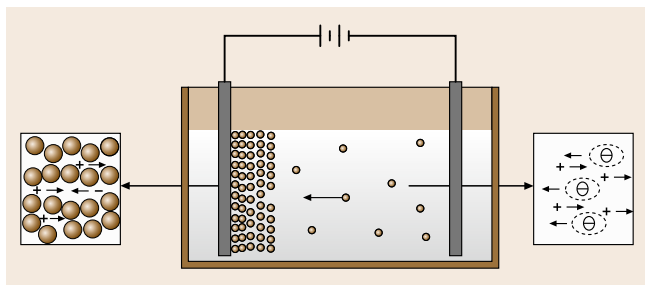
Upon the application of an external electric field, charged particles are set in motion, as schematically illustrated in Fig. 5.8 [5.59]. This type of motion is referred to as electrophoresis. When a charged particle moves, some of the solvent or solution surrounding the particle will also move with it, since part of the solvent or solution is tightly bound to the particle. The plane that separates the tightly bound liquid layer from the rest of the liquid is called the *slip plane* (Fig. 5.7). The electric potential at the slip plane is known as the *zeta potential*, which is an important parameter when determining the stability and transport of a colloidal dispersion or a sol. A zeta potential of more than about 25 mV is typically required to stabilize a system [5.60]. The zeta potential ζ around a spherical particle can be described using the relation [5.61]

$$\zeta = \frac{Q}{4\pi\varepsilon_r a\,(1+\kappa a)}$$

with

$$\kappa = \left(\frac{e^2 \sum n_i z_i^2}{\varepsilon_r \varepsilon_0 k_B T}\right)^{1/2} , \tag{5.4}$$

Fig. 5.8 Schematic showing electrophoresis. Upon application of an external electric field to a colloidal system or a sol, the charged nanoparticles or nanoclusters are set in motion (after [5.1])

where Q is the charge on the particle, a is the radius of the particle out to the shear plane, ε_r is the relative dielectric constant of the medium, and n_i and z_i are the

bulk concentration and valence of the i-th ion in the system, respectively.

The mobility of a nanoparticle in a colloidal dispersion or a sol μ, is dependent on the dielectric constant of the liquid medium ε_r, the zeta potential of the nanoparticle ζ, and the viscosity η of the fluid. Several forms for this relationship have been proposed, such as the Hückel equation [5.59, 61, 63–65]

$$\mu = \frac{2\varepsilon_r\varepsilon_0\zeta}{3\pi\eta} . \tag{5.5}$$

Electrophoretic deposition simply uses the oriented motion of charged particles in an electrical field to grow films or monoliths by transferring the solid particles from a colloidal dispersion or a sol onto the surface

of an electrode. If the particles are positively charged (or more precisely, they have a positive zeta potential), deposition of solid particles will occur at the cathode. Otherwise, deposition will be at the anode. The electrostatic double layers collapse at the electrodes and the particles coagulate, producing porous materials made of compacted nanoparticles. Typical packing densities are far less than the theoretical density of 74 vol.% [5.66]. Many theories have been proposed to explain the processes at the deposition surface during electrophoretic deposition. However, the evolution of structure on the deposition surface is not well understood. The electrochemical processes that take place at the deposition surface and at the electrodes are complex and vary from system to system. The final density is dependent upon
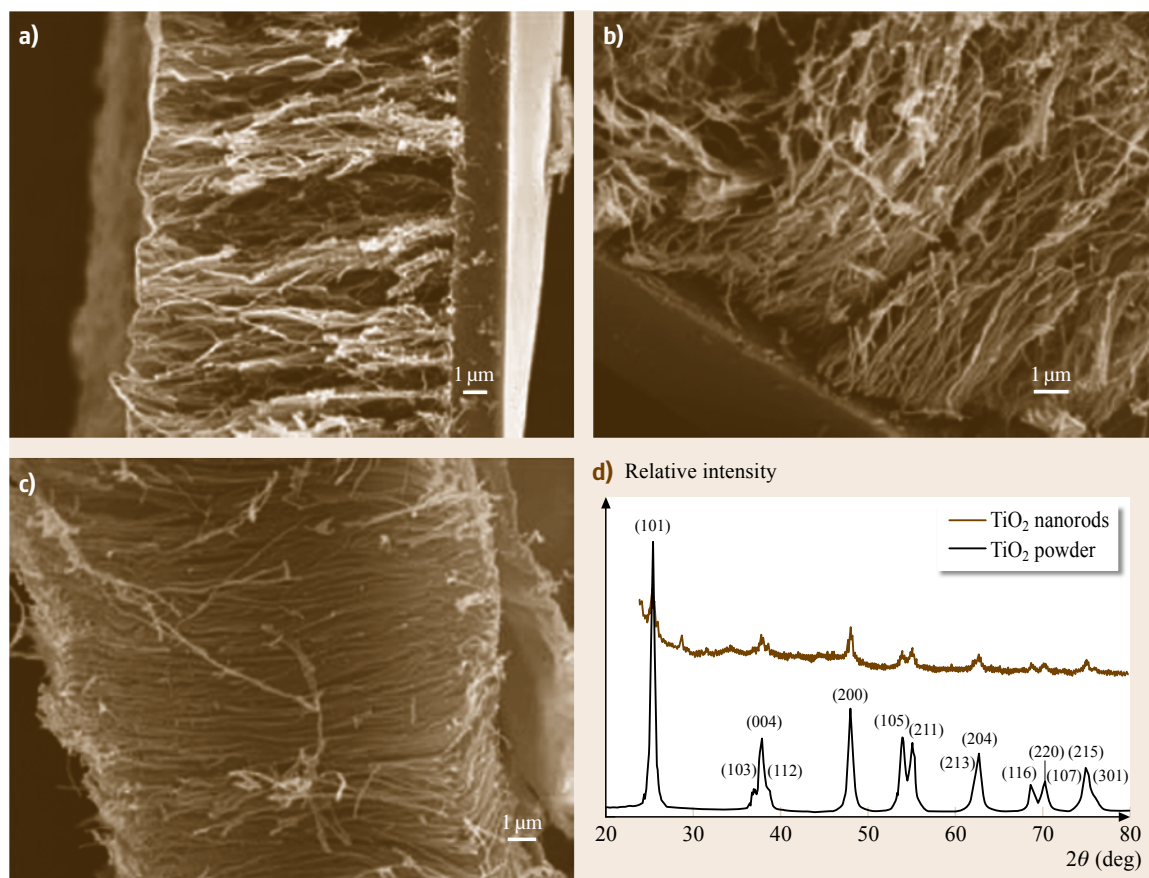
Fig. 5.9a–d SEM micrograph of TiO$_2$ nanorods grown by template-based electrochemically induced sol–gel deposition. The diameters of the nanorods are approximately: **(a)** 180 nm (for the 200 nm polycarbonate membrane); **(b)** 90 nm (for the 100 nm membrane); **(c)** 45 nm (for the 50 nm membrane). **(d)** XRD patterns of both the grown nanorods and a powder derived from the same sol. Both samples consist of the anatase phase only and no peak position shift was observed (after [5.62])

the concentration of particles in sols or colloidal dispersions, the zeta potential, the external electric field, and the reaction kinetics between the surfaces of the particles. A slow reaction and a slow arrival of nanoparticles onto the surface would allow sufficient particle relaxation on the deposition surface, so a high packing density would be expected.

5.3.1 Polycrystalline Oxides

Limmer et al. [5.62, 67–69] combined sol–gel preparation with electrophoretic deposition to prepare nanorods of various complex oxides. One of the advantages of this technique is the ability to synthesize complex oxides and organic–inorganic hybrids with desired stoichiometric compositions. Another advantage is their applicability to a variety of materials. In their approach, conventional sol–gel processing was applied to the synthesis of various sols. By controlling the sol preparation appropriately, nanometer particles of a desired stoichiometric composition were formed, and electrostatically stabilized by pH adjustment. Using radiation-tracked etched polycarbonate membranes with an electric field of ≈ 1.5 V/cm, they have grown nanowires with diameters ranging from 40 to 175 nm and lengths of $10 \, \mu\text{m}$, corresponding to the thickness of the membrane. The materials include anatase TiO_2, amorphous SiO_2, perovskite $BaTiO_3$ and $Pb(Ti, Zr)O_3$, and layered perovskite $Sr_2Nb_2O_7$. Figure 5.9 shows SEM micrographs and XRD patterns of TiO_2 nanorod arrays [5.62].

Wang et al. [5.70] used electrophoretic deposition to make nanorods of ZnO from colloidal sols. ZnO colloidal sol was prepared by hydrolyzing an alcoholic solution of zinc acetate with NaOH, with a small amount of zinc nitrate added as a binder. This solution was then introduced into the pores of anodic alumina membranes at voltages of 10–400 V. It was found that lower voltages led to dense, solid nanorods, while higher voltages caused the formation of hollow tubules. They suggested that the higher voltages cause dielectric breakdown of the anodic alumina, causing it to become as positively charged as the cathode. Electrostatic attraction between the ZnO nanoparticles and the pore walls then leads to tubule formation.

5.3.2 Single Crystal Oxide Nanorod Arrays Obtained by Changing the Local pH

A modified version of sol electrophoretic deposition has been used to grow single crystalline titanium oxide and vanadium pentoxide nanorod arrays from TiO^{2+} and VO_2^+ solutions respectively. *Miao* et al. [5.71] prepared single crystalline TiO_2 nanowires by electrochemically induced sol–gel deposition. Titania electrolyte solution was prepared by dissolving Ti powder into a H_2O_2 and NH_4OH aqueous solution to form TiO^{2+} ionic clusters [5.72]. When an electric field was applied, the TiO^{2+} ionic clusters diffused to the cathode and underwent hydrolysis and condensation reactions, resulting in the deposition of nanorods of amorphous TiO_2 gel. After heating at $240\,°\text{C}$ for 24 h in air, single crystal anatase nanorods with diameters of 10, 20, and 40 nm and lengths ranging from 2 to $10 \, \mu\text{m}$ were synthesized. The formation of single crystal TiO_2 nanorods here is different to that reported by *Martin*'s group [5.73]. It is suggested that the nanoscale crystallites generated during heating assembled epitaxially to form single crystal nanorods.

During typical sol–gel processing, nanoclusters are formed through homogeneous nucleation and subsequent growth through sequential yet parallel hydrolysis and condensation reactions. Sol electrophoretic deposition enriches and deposits these formed nanoclusters at an appropriate electrode surface under an external electric field. The modified process is to limit and induce the condensation reaction at the growth surface by changing local pH value, which is a result of partial water hydrolysis at the electrode or growth surface

$$2H_2O + 2e^- \rightarrow H_2 + 2OH^- \, , \qquad (5.6)$$
$$2VO_2^+ + 2OH^- \rightarrow V_2O_5 + H_2O \, . \qquad (5.7)$$
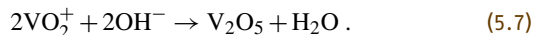
Reaction (5.6), or the electrolysis of water, plays a very important role here. As the reaction proceeds, hydroxyl groups are produced, resulting in increased pH near to the deposition surface. This increase in pH value near to the growth surface initiated and promotes the precipitation of V_2O_5, or reaction (5.7). The initial pH of the VO_2^+ solution is ≈ 1.0, meaning that VO_2^+ is stable. However, when the pH increases to ≈ 1.8, VO_2^+ is no longer stable and solid V_2O_5 forms. Since the change in pH occurs near to the growth surface, reaction (5.7) or deposition is likely to occur on the surface of the electrode through heterogeneous nucleation and subsequent growth. It should be noted that the hydrolysis of water has another effect on the deposition of solid V_2O_5. Reaction (5.6) produces hydrogen on the growth surface. These molecules may poison the growth surface before dissolving into the electrolyte or by forming a gas bubble, which may cause the formation of porous nanorods.
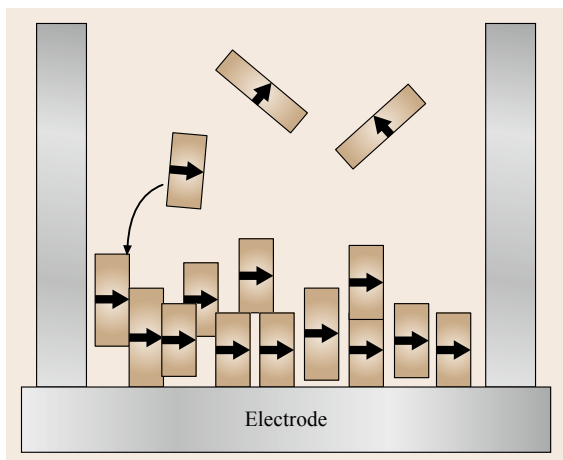
The formation of single crystal nanorods from solutions by pH change-induced surface condensation has been proven by TEM analyses, including high-resolution imaging showing the lattice fringes and electron diffraction. The growth of single crystal nanorods by pH change-induced surface condensation is attributed to evolution selection growth, which is briefly summarized below. The initial heterogeneous nucleation or deposition onto the substrate surface results in the formation of nuclei with random orientations. The subsequent growth of various facets of a nucleus is dependent on the surface energy, and varies significantly from one facet to another [5.74]. For one-dimensional growth, such as film growth, only the highest growth rate with a direction perpendicular to the growth surface will be able to continue to grow. The nuclei with the fastest growth direction perpendicular to the growth surface will grow larger, while nuclei with slower growth rates will eventually cease to grow. Such a growth mechanism results in the formation of columnar structured films where all of the grains have the same crystal orientation (known as textured films) [5.75, 76]. In the case of nanorod growth inside a pore channel, such evolution selection growth is likely to lead to the formation of a single crystal nanorod or a bundle of single crystal nanorods per pore channel. Figure 5.10 shows typical TEM micrographs and selected-area electron diffraction patterns of V_2O_5 nanorods. It is well known that [010] (the b-axis) is the fastest growth direction for a V_2O_5 crystal [5.77, 78], which would explain why single crystal vanadium nanorods or a bundle of single crystal nanorods grow along the b-axis.

5.3.3 Single Crystal Oxide Nanorod Arrays Grown by Homoepitaxial Aggregation

Single crystal nanorods can also be grown directly by conventional electrophoretic deposition. However, several requirements must be met for such growth. First, the nanoclusters or particles in the sol must have a crystalline structure extended to the surface. Second, the deposition of nanoclusters on the growth surface must have a certain degree of reversibility so that the nanoclusters can rotate or reposition prior to their irreversible incorporation into the growth surface. Thirdly, the deposition rate must be slow enough to permit sufficient time for the nanoclusters to rotate or reposition. Lastly, the surfaces of the nanoclusters must be free of strongly attached alien chemical species. Although precise control of all these parameters remains a challenge, the growth of single crystal nanorods through homoepitaxial aggregation of nanocrystals has been demonstrated [5.79, 80]. The formation of single crystalline vanadium pentoxide nanorods by template-based sol electrophoretic deposition can be attributed to homoepitaxial aggregation of crystalline nanoparticles. Thermodynamically it is favorable for the crystalline nanoparticles to aggregate epitaxially; this growth behavior and mechanism is well documented in the literature [5.81, 82]. In this growth mechanism, an initial weak interaction between two nanoparticles allows rotation and migration relative to each other. Obviously, homoepitaxial aggregation is a competitive process and porous structure is expected to form through this homoepitaxial aggregation (as schematically illustrated in Fig. 5.11). Vanadium oxide particles present in a typ-
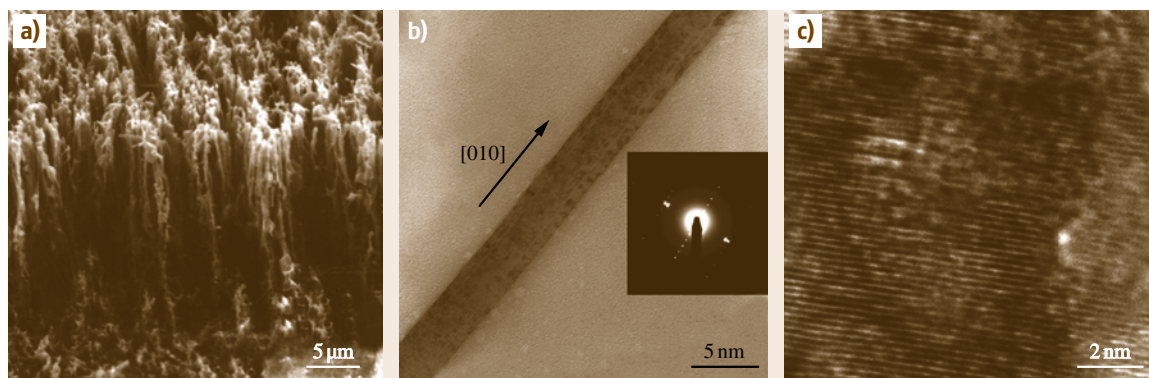
Fig. 5.10 (a) SEM image of V_2O_5 nanorod arrays on an ITO substrate grown in a 200 nm carbonate membrane by sol electrophoretic deposition; **(b)** TEM image of a V_2O_5 nanorod with its electron diffraction pattern; **(c)** high-resolution TEM image of the V_2O_5 nanorod showing the lattice fringes (after [5.54])

Fig. 5.11 Schematic illustration of the homoepitaxial aggregation growth mechanism of single-crystalline nanorods (after [5.54])

ical sol are known to easily form ordered crystalline structure [5.83], so it is reasonable to expect that homoepitaxial aggregation of vanadium nanocrystals from sol results in the formation of single crystal nanorods. Single crystal nanorods formed in this way are likely to undergo significant shrinkage when fired at high temperatures due to its original porous nature; 50% lateral shrinkage has been observed in vanadium pentoxide nanorods formed by this method. In addition, it might

be possible that the electric field and the internal surfaces of the pore channels play significant roles in the orientation of the nanorods, as suggested in the literature [5.84, 85].

5.3.4 Nanowires and Nanotubes of Fullerenes and Metallofullerenes

Electrophoretic deposition in combination with template-based growth has also been successfully explored in the formation of nanowires and nanotubes of carbon fullerenes, such as C_{60} [5.86], or metallofullerenes, such as $Sc@C_{82}(I)$ [5.87]. Typical experiments include the purification or isolation of the fullerenes or metallofullerenes required using multiple-step liquid chromatography and dispersion of the fullerenes in a mixed solvent of acetonitrile/toluene in a ratio of $7:1$. The electrolyte solution has a relatively low concentration of fullerenes ($35\,\mu M$) and metallofullerenes ($40\,\mu M$), and the electrophoretic deposition takes place with an externally applied electric field of 100–$150\,V$ with a distance of $5\,mm$ between the two electrodes. Both nanorods and nanotubes of fullerenes or metallofullerenes can form and it is believed that initial deposition occurs along the pore surface. A short deposition time results in the formation of nanotubes, whereas extended deposition leads to the formation of solid nanorods. These nanorods possess either crystalline or amorphous structure.

5.4 Template Filling

Directly filling a template with a liquid mixture precursor is the most straightforward and versatile method for preparing nanowire or nanorod arrays. The drawback of this approach is that it is difficult to ensure complete filling of the template pores. Both nanorods and nanotubules can be obtained depending on the interfacial adhesion and the solidification modes. If the adhesion between the pore walls and the filling material is weak, or if solidification starts at the center (or from one end of the pore, or uniformly throughout the rods), solid nanorods are likely to form. If the adhesion is strong, or if the solidification starts at the interfaces and proceeds inwardly, hollow nanotubules are likely to form.

5.4.1 Colloidal Dispersion (Sol) Filling

Martin and coworkers [5.73, 88] have studied the formation of various oxide nanorods and nanotubules by

simply filling the templates with colloidal dispersions (Fig. 5.12). Nanorod arrays of a mesoporous material (SBA-15) were recently synthesized by filling an ordered porous alumina membrane with sol containing surfactant (Pluronic P123) [5.89]. Colloidal dispersions were prepared using appropriate sol–gel processing techniques. The template was placed in a stable sol for various periods of time. The capillary force drives the sol into the pores if the sol has good wettability for the template. After the pores were filled with sol, the template was withdrawn from the sol and dried. The sample was fired at elevated temperatures to remove the template and to densify the sol–gel-derived green nanorods.

A sol typically consists of a large volume fraction of solvent, up to 90% or higher. Although the capillary force may ensure complete filling of the pores with the suspension, the amount of solid occupying the pore space is small. Upon drying and subsequent fir-
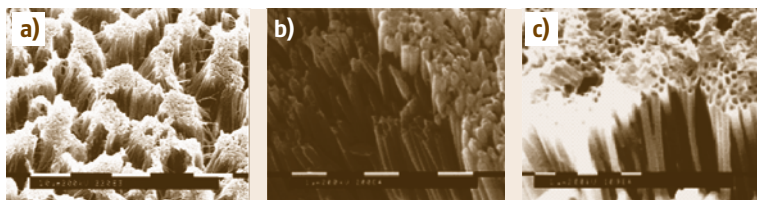
Fig. 5.12a–c SEM micrographs of oxide nanorods created by filling the templates with sol–gels: **(a)** ZnO, **(b)** TiO$_2$ and **(c)** hollow nanotube (after [5.73])

ing processes, significant shrinkage would be expected. However, the actual shrinkage observed is small when compared with the pore size. These results indicate that an (unknown) mechanism is acting to enrich the concentration of solid inside the pores. One possible mechanism could be the diffusion of solvent through the membrane, leading to the enrichment of solid on the internal surfaces of the template pores, similar to what happens during ceramic slip casting [5.90]. Figure 5.12a is a top view of ZnO nanotubules array, Fig. 5.12b is TiO$_2$ nanotubules array, Fig. 5.12c is hollow nanotube array. The observed formation of nanotubules (in Fig. 5.12 [5.73]) may imply that this process is indeed present. However, considering the fact that the templates were typically emerged into sol for just a few minutes, diffusion through the membrane and enrichment of the solid inside the pores must be rather rapid processes. It was also noticed that the nanorods made by template filling are commonly polycrystalline or amorphous, although single crystal TiO$_2$ nanorods were sometimes observed for nanorods smaller than 20 nm [5.73].

5.4.2 Melt and Solution Filling

Metallic nanowires can also be synthesized by filling a template with molten metals [5.91]. One example is the preparation of bismuth nanowires using pressure injection of molten bismuth into the nanochannels of an anodic alumina template [5.92]. The anodic alumina template was degassed and immersed in the liquid bismuth at 325 °C ($T_m = 271.5$ °C for Bi), and then high pressure Ar gas of ≈ 300 bar was applied in order to inject liquid Bi into the nanochannels of the template for 5 h. Bi nanowires with diameters of 13–110 nm and large aspect ratios (of up to several hundred) have been obtained. Individual nanowires are believed to be single-crystal. When exposed to air, bismuth nanowires are readily oxidized. An amorphous oxide layer ≈ 4 nm in thickness was observed after 48 h. After 4 weeks, the bismuth nanowires were completely oxidized. Nanowires of other metals, such as In, Sn and Al, and the semiconductors Se, Te, GaSb, and Bi$_2$Te$_3$, were also

prepared by injecting molten liquid into anodic alumina templates [5.93].

Polymeric fibrils have been made by filling the template pores with a monomer solution containing the desired monomer and a polymerization reagent, followed by in situ polymerization [5.14, 94–97]. The polymer preferentially nucleates and grows on the pore walls, resulting in tubules at short deposition times.

Metal, oxide and semiconductor nanowires have recently been synthesized using self-assembled mesoporous silica as the template. For example, *Han* et al. [5.98] have synthesized Au, Ag and Pt nanowires in mesoporous silica templates. The mesoporous templates were first filled with aqueous solutions of the corresponding metal salts (such as HAuCl$_4$). After drying and treatment with CH$_2$Cl$_2$, the samples were reduced under H$_2$ flow to form metallic nanowires. *Liu* et al. [5.99] carefully studied the interface between these nanowires and the matrix using high-resolution electron microscopy and electron energy loss spectroscopy techniques. A sharp interface only exists between noble metal nanowires and the matrix. For magnetic nickel oxide, a core–shell nanorod structure containing a nickel oxide core and a thin nickel silicate shell was observed. The magnetic properties of the templated nickel oxide were found to be significantly different from nickel oxide nanopowders due to the alignment of the nanorods. In another study, *Chen* et al. filled the pores of a mesoporous silica template with an aqueous solution of Cd and Mn salts, dried the sample, and reacted it with H$_2$S gas to convert it to (Cd,Mn)S [5.100].

5.4.3 Centrifugation

Filling the template with nanoclusters via centrifugation forces is another inexpensive method for mass producing nanorod arrays. Figure 5.13 shows SEM images of lead zirconate titanate (PZT) nanorod arrays with uniform sizes and unidirectional alignment [5.101]. These nanorod arrays were grown in polycarbonate membrane from PZT sol by centrifugation at 1500 rpm for 60 min. The samples were attached to silica glass
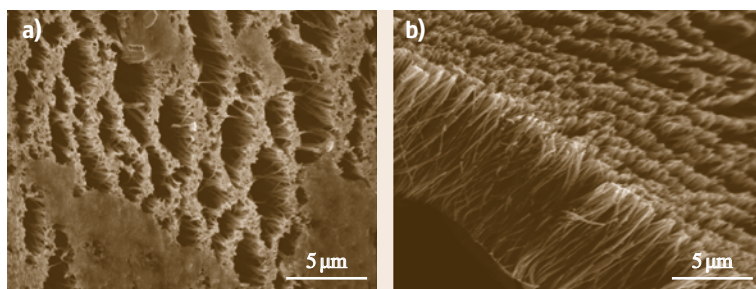
Fig. 5.13a,b SEM images of the top view (*left*) and side view (*right*) of lead zirconate titanate (PZT) nanorod arrays grown in polycarbonate membrane from PZT sol by centrifugation at 1500 rpm for 60 min. Samples were attached to silica glass and fired at 650 °C in air for 60 min (after [5.101])

and fired at 650 °C in air for 60 min. Nanorod arrays of other oxides (silica and titania) were prepared. The advantages of centrifugation include its applicability to any colloidal dispersion system, including those consisting of electrolyte-sensitive nanoclusters or molecules.

5.5 Converting from Reactive Templates

Nanorods or nanowires can also be synthesized using consumable templates, although the resultant nanowires and nanorods are generally not ordered to form aligned arrays. Nanowires of compounds can be prepared using a template-directed reaction. First nanowires or nanorods of one constituent element are prepared, and then these are reacted with chemicals containing the other element desired in order to form the final product. *Gates* et al. [5.102] converted single crystalline trigonal selenium nanowires into single crystalline nanowires of Ag_2Se by reacting Se nanowires with aqueous $AgNO_3$ solutions at room temperature. Nanorods can also be synthesized by reacting volatile metal halides or oxide species with carbon nanotubes to form solid carbide nanorods with diameters of between 2 and 30 nm and lengths of up to 20 μm [5.103]. ZnO nanowires were prepared by oxidizing metallic zinc nanowires [5.104]. Hollow nanotubules of $MoS_2 \approx 30$ μm long and 50 nm in external diameter with wall thicknesses of 10 nm were prepared

by filling a solution mixture of the molecular precursors, $(NH_4)_2MoS_4$ and $(NH_4)_2Mo_3S_{13}$, into the pores of alumina membrane templates. Then the template filled with the molecular precursors was heated to an elevated temperature and the molecular precursors were thermally decomposed into MoS_2 [5.105]. Certain polymers and proteins were also used to direct the growth of nanowires of metals or semiconductors. For example, *Braun* et al. [5.106] reported a two-step procedure using DNA as a template for the vectorial growth of a silver nanorods 12 μm in length and 100 nm in diameter. CdS nanowires were prepared by polymer-controlled growth [5.107]. For the synthesis of CdS nanowires, cadmium ions were well distributed in a polyacrylamide matrix. The Cd^{2+}-containing polymer was treated with thiourea (NH_2CSNH_2) solvothermally in ethylenediamine at 170 °C, resulting in degradation of polyacrylamide. Single crystal CdS nanowires 40 nm in diameter and up to 100 μm in length were obtained with preferential [001] orientations.

5.6 Summary and Concluding Remarks

This chapter provides a brief summary of the fundamentals of and techniques used for the template-based synthesis of nanowire or nanorod arrays. Examples were used to illustrate the growth of each nanorod material made with each technique. The literature associated with this field is overwhelming and is expanding very rapidly. This chapter is by no means compre-

hensive in its coverage of the relevant literature. Four groups of template-based synthesis methods have been reviewed and discussed in detail. Electrochemical deposition or electrodeposition is the method used to grow electrically conductive or semiconductive materials, such as metals, semiconductors, and conductive polymers and oxides. Electrophoretic deposition from

colloidal dispersion is the method used to synthesize dielectric nanorods and nanowires. Template filling is conceptually straightforward, although complete filling is often very difficult. Converting reactive templates is a method used to achieve both nanorod arrays and randomly oriented nanowires or nanorods, and it is often combined with other synthetic methods.

This chapter has focused on the growth of solid nanorod and nanowire arrays by template-based synthesis; however, the use of template-based synthesis to synthesize nanotubes, and in particular nanotube arrays, has received increasing attention [5.108]. One of the greatest advantages using template-based synthesis to grow of nanotubes and nanotube arrays is the independent control of the lengths, diameters, and the wall thicknesses of the nanotubes available. While the lengths and the diameters of the resultant nanotubes are dependent on the templates used for the synthesis, the wall thicknesses of the nanotubes can be readily controlled through the duration of growth. Another great advantage of the template-based synthesis of nanotubes is the possibility of multilayered hollow nanotube or solid nanocable structures. For example, $Ni@V_2O_5 \cdot nH_2O$ nanocable arrays have been synthesized by a two-step approach [5.109]. First, Ni nanorod arrays were grown in a PC template by electrochemical deposition, and then the PC template was removed by pyrolysis, followed by sol electrophoretic deposition of $V_2O_5 \cdot nH_2O$ on the surfaces of the Ni nanorod arrays. It is obvious that there is a lot of scope for more research into template-based syntheses of nanorod, nanotube and nanocable arrays, and their applications.

References

5.1 G.Z. Cao: *Nanostructures and Nanomaterials: Synthesis, Properties and Applications* (Imperial College, London 2004)

5.2 Z.L. Wang: *Nanowires and Nanobelts: Materials, Properties and Devices, Nanowires and Nonobelts of Functional Materials*, Vol. 2 (Kluwer, Boston 2003)

5.3 Y. Xia, P. Yang, Y. Sun, Y. Wu, Y. Yin, F. Kim, H. Yan: One-dimensional nanostructures: Synthesis, characterization and applications, Adv. Mater. **15**, 353–389 (2003)

5.4 A. Huczko: Template-based synthesis of nanomaterials, Appl. Phys. A **70**, 365–376 (2000)

5.5 C. Burda, X. Chen, R. Narayanan, M.A. El-Sayed: Chemistry and properties of nanocrystals of different shapes, Chem. Rev. **105**, 1025–1102 (2005)

5.6 X. Duan, C.M. Lieber: General synthesis of compound semiconductor nanowires, Adv. Mater. **12**, 298–302 (2000)

5.7 M.P. Zach, K.H. Ng, R.M. Penner: Molybdenum nanowires by electrodeposition, Science **290**, 2120–2123 (2000)

5.8 R.C. Furneaux, W.R. Rigby, A.P. Davidson: The formation of controlled-porosity membranes from anodically oxidized aluminium, Nature **337**, 147–149 (1989)

5.9 R.L. Fleisher, P.B. Price, R.M. Walker: *Nuclear Tracks in Solids* (Univ. of California Press, Berkeley 1975)

5.10 R.J. Tonucci, B.L. Justus, A.J. Campillo, C.E. Ford: Nanochannel array glass, Science **258**, 783–787 (1992)

5.11 G.E. Possin: A method for forming very small diameter wires, Rev. Sci. Instrum. **41**, 772–774 (1970)

5.12 C. Wu, T. Bein: Conducting polyaniline filaments in a mesoporous channel host, Science **264**, 1757–1759 (1994)

5.13 S. Fan, M.G. Chapline, N.R. Franklin, T.W. Tombler, A.M. Cassell, H. Dai: Self-oriented regular arrays of carbon nanotubes and their field emission properties, Science **283**, 512–514 (1999)

5.14 P. Enzel, J.J. Zoller, T. Bein: Intrazeolite assembly and pyrolysis of polyacrylonitrile, J. Chem. Soc. Chem. Commun. **8**, 633–635 (1992)

5.15 C. Guerret-Piecourt, Y. Le Bouar, A. Loiseau, H. Pascard: Relation between metal electronic structure and morphology of metal compounds inside carbon nanotubes, Nature **372**, 761–765 (1994)

5.16 P.M. Ajayan, O. Stephan, P. Redlich, C. Colliex: Carbon nanotubes as removable templates for metal oxide nanocomposites, nanostructures, Nature **375**, 564–567 (1995)

5.17 M. Knez, A.M. Bittner, F. Boes, C. Wege, H. Jeske, E. Maiâ, K. Kern: Biotemplate synthesis of 3-nm nickel and cobalt nanowires, Nano Lett. **3**, 1079–1082 (2003)

5.18 R. Gasparac, P. Kohli, M.O.M.L. Trofin, C.R. Martin: Template synthesis of nano test tubes, Nano Lett. **4**, 513–516 (2004)

5.19 C.F. Monson, A.T. Woolley: DNA-templated construction of copper nanowires, Nano Lett. **3**, 359–363 (2003)

5.20 Y. Weizmann, F. Patolsky, I. Popov, I. Willner: Telomerase-generated templates for the growing of metal nanowires, Nano Lett. **4**, 787–792 (2004)

5.21 A. Despic, V.P. Parkhuitik: *Modern Aspects of Electrochemistry*, Vol. 20 (Plenum, New York 1989)

5.22 D. Al Mawiawi, N. Coombs, M. Moskovits: Magnetic properties of Fe deposited into anodic aluminum oxide pores as a function of particle size, J. Appl. Phys. **70**, 4421–4425 (1991)

5.23 C.A. Foss, M.J. Tierney, C.R. Martin: Template-synthesis of infrared-transparent metal microcylin-

ders: Comparison of optical properties with the predictions of effective medium theory, J. Phys. Chem. **96**, 9001–9007 (1992)

5.24 A.J. Bard, L.R. Faulkner: *Electrochemical Methods* (Wiley, New York 1980)

5.25 J.B. Mohler, H.J. Sedusky: *Electroplating for the Metallurgist, Engineer and Chemist* (Chemical Publishing, New York 1951)

5.26 T.M. Whitney, J.S. Jiang, P.C. Searson, C.L. Chien: Fabrication and magnetic properties of arrays of metallic nanowires, Science **261**, 1316–1319 (1993)

5.27 F.R.N. Nabarro, P.J. Jackson: Growth of crystal whiskers – A review. In: *Growth and Perfection of Crystals*, ed. by R.H. Doremus, B.W. Roberts, D. Turnbull (Wiley, New York 1958) pp. 11–102

5.28 B.Z. Tang, H. Xu: Preparation, alignment and optical properties of soluble poly(phenylacetylene)-wrapped carbon nanotubes, Macromolecules **32**, 2567–2569 (1999)

5.29 W.D. Williams, N. Giordano: Fabrication of 80 Å metal wires, Rev. Sci. Instrum. **55**, 410–412 (1984)

5.30 C.G. Jin, G.W. Jiang, W.F. Liu, W.L. Cai, L.Z. Yao, Z. Yao, X.G. Li: Fabrication of large-area single crystal bismuth nanowire arrays, J. Mater. Chem. **13**, 1743–1746 (2003)

5.31 M.E.T. Molares, V. Buschmann, D. Dobrev, R. Neumann, R. Scholz, I.U. Schuchert, J. Vetter: Single-crystalline copper nanowires produced by electrochemical deposition in polymeric ion track membranes, Adv. Mater. **13**, 62–65 (2001)

5.32 G. Yi, W. Schwarzacher: Single crystal superconductor nanowires by electrodeposition, Appl. Phys. Lett. **74**, 1746–1748 (1999)

5.33 C.J. Brumlik, V.P. Menon, C.R. Martin: Synthesis of metal microtubule ensembles utilizing chemical, electrochemical and vacuum deposition techniques, J. Mater. Res. **268**, 1174–1183 (1994)

5.34 C.J. Brumlik, C.R. Martin: Template synthesis of metal microtubules, J. Am. Chem. Soc. **113**, 3174–3175 (1991)

5.35 C.J. Miller, C.A. Widrig, D.H. Charych, M. Majda: Microporous aluminum oxide films at electrodes. 4. Lateral charge transport in self-organized bilayer assemblies, J. Phys. Chem. **92**, 1928–1936 (1988)

5.36 W. Han, S. Fan, Q. Li, Y. Hu: Synthesis of gallium nitride nanorods through a carbon nanotube-confined reaction, Science **277**, 1287–1289 (1997)

5.37 G.O. Mallory, J.B. Hajdu (Eds.): *Electroless Plating: Fundamentals and Applications* (AESF, Orlando 1990)

5.38 C. Schönenberger, B.M.I. van der Zande, L.G.J. Fokkink, M. Henny, C. Schmid, M. Krüger, A. Bachtold, R. Huber, H. Birk, U. Staufer: Template synthesis of nanowires in porous polycarbonate membranes: Electrochemistry and morphology, J. Phys. Chem. B **101**, 5497–5505 (1997)

5.39 J.D. Klein, R.D. Herrick II, D. Palmer, M.J. Sailor, C.J. Brumlik, C.R. Martin: Electrochemical fabrica-

tion of cadmium chalcogenide microdiode arrays, Chem. Mater. **5**, 902–904 (1993)

5.40 L.D. Hicks, M.S. Dresselhaus: Thermoelectric figure of merit of a one-dimensional conductor, Phys. Rev. B **47**, 679–682 (1993)

5.41 M.S. Dresselhaus, G. Dresselhaus, X. Sun, Z. Zhang, S.B. Cronin, T. Koga: Low-dimensional thermoelectric materials, Phys. Solid State **41**, 679–682 (1999)

5.42 M.S. Sander, R. Gronsky, T. Sands, A.M. Stacy: Structure of bismuth telluride nanowire arrays fabricated by electrodeposition into porous anodic alumina templates, Chem. Mater. **15**, 335–339 (2003)

5.43 C. Lin, X. Xiang, C. Jia, W. Liu, W. Cai, L. Yao, X. Li: Electrochemical fabrication of large-area, ordered Bi_2Te_3 nanowire arrays, J. Phys. Chem. B **108**, 1844–1847 (2004)

5.44 D.S. Xu, Y.J. Xu, D.P. Chen, G.L. Guo, L.L. Gui, Y.Q. Tang: Preparation of CdS single-crystal nanowires by electrochemically induced deposition, Adv. Mater. **12**, 520–522 (2000)

5.45 C. Lin, G. Zhang, T. Qian, X. Li, Z. Yao: Large-area Sb_2Te_3 nanowire arrays, J. Phys. Chem. B **109**, 1430–1432 (2005)

5.46 C. Jérôme, R. Jérôme: Electrochemical synthesis of polypyrrole nanowires, Angew. Chem. Int. Ed. **37**, 2488–2490 (1998)

5.47 A.G. MacDiarmid: Nobel lecture: "Synthetic metals": A novel role for organic polymers, Rev. Mod. Phys. **73**, 701–712 (2001)

5.48 K. Doblhofer, K. Rajeshwar: *Handbook of Conducting Polymers* (Marcel Dekker, New York 1998), Chap. 20

5.49 L. Dauginet, A.-S. Duwez, R. Legras, S. Demoustier-Champagne: Surface modification of polycarbonate and poly(ethylene terephthalate) films and membranes by polyelectrolyte, Langmuir **17**, 3952–3957 (2001)

5.50 C.R. Martin: Membrane-based synthesis of nanomaterials, Chem. Mater. **8**, 1739–1746 (1996)

5.51 C.R. Martin: Template synthesis of polymeric and metal microtubules, Adv. Mater. **3**, 457–459 (1991)

5.52 J.C. Hulteen, C.R. Martin: A general template-based method for the preparation of nanomaterials, J. Mater. Chem. **7**, 1075–1087 (1997)

5.53 L. Liang, J. Liu, C.F. Windisch Jr., G.J. Exarhos, Y. Lin: Assembly of large arrays of oriented conducting polymer nanowires, Angew. Chem. Int. Ed. **41**, 3665–3668 (2002)

5.54 K. Takahashi, S.J. Limmer, Y. Wang, G.Z. Cao: Growth and electrochemical properties of single-crystalline V_2O_5 nanorod arrays, Jpn. J. Appl. Phys. B **44**, 662–668 (2005)

5.55 M.J. Zheng, L.D. Zhang, G.H. Li, W.Z. Shen: Fabrication and optical properties of large-scale uniform zinc oxide nanowire arrays by one-step electrochemical deposition technique, Chem. Phys. Lett. **363**, 123–128 (2002)

5.56 I. Zhitomirsky: Cathodic electrodeposition of ceramic and organoceramic materials. Fundamental aspects, Adv. Colloid Interf. Sci. **97**, 279–317 (2002)

5.57 O.O. Van der Biest, L.J. Vandeperre: Electrophoretic deposition of materials, Annu. Rev. Mater. Sci. **29**, 327–352 (1999)

5.58 P. Sarkar, P.S. Nicholson: Electrophoretic deposition (EPD): Mechanism, kinetics, and application to ceramics, J. Am. Ceram. Soc. **79**, 1987–2002 (1996)

5.59 A.C. Pierre: *Introduction to Sol-Gel Processing* (Kluwer, Norwell 1998)

5.60 J.S. Reed: *Introduction to the Principles of Ceramic Processing* (Wiley, New York 1988)

5.61 R.J. Hunter: *Zeta Potential in Colloid Science: Principles and Applications* (Academic, London 1981)

5.62 S.J. Limmer, T.P. Chou, G.Z. Cao: A study on the growth of TiO_2 using sol electrophoresis, J. Mater. Sci. **39**, 895–901 (2004)

5.63 C.J. Brinker, G.W. Scherer: *Sol-Gel Science: the Physics and Chemistry of Sol-Gel Processing* (Academic, San Diego 1990)

5.64 J.D. Wright, N.A.J.M. Sommerdijk: *Sol-Gel Materials: Chemistry and Applications* (Gordon and Breach, Amsterdam 2001)

5.65 D.H. Everett: *Basic Principles of Colloid Science* (The Royal Society of Chemistry, London 1988)

5.66 W.D. Callister: *Materials Science and Engineering: An Introduction* (Wiley, New York 1997)

5.67 S.J. Limmer, S. Seraji, M.J. Forbess, Y. Wu, T.P. Chou, C. Nguyen, G.Z. Cao: Electrophoretic growth of lead zirconate titanate nanorods, Adv. Mater. **13**, 1269–1272 (2001)

5.68 S.J. Limmer, S. Seraji, M.J. Forbess, Y. Wu, T.P. Chou, C. Nguyen, G.Z. Cao: Template-based growth of various oxide nanorods by sol-gel electrophoresis, Adv. Funct. Mater. **12**, 59–64 (2002)

5.69 S.J. Limmer, G.Z. Cao: Sol-gel electrophoretic deposition for the growth of oxide nanorods, Adv. Mater. **15**, 427–431 (2003)

5.70 Y.C. Wang, I.C. Leu, M.N. Hon: Effect of colloid characterics on the fabrication of ZnO nanowire arrays by electrophoretic deposition, J. Mater. Chem. **12**, 2439–2444 (2002)

5.71 Z. Miao, D. Xu, J. Ouyang, G. Guo, Z. Zhao, Y. Tang: Electrochemically induced sol-gel preparation of single-crystalline TiO_2 nanowires, Nano Lett. **2**, 717–720 (2002)

5.72 C. Natarajan, G. Nogami: Cathodic electrodeposition of nanocrystalline titanium dioxide thin films, J. Electrochem. Soc. **143**, 1547–1550 (1996)

5.73 B.B. Lakshmi, P.K. Dorhout, C.R. Martin: Sol-gel template synthesis of semiconductor nanostructures, Chem. Mater. **9**, 857–863 (1997)

5.74 A. van der Drift: Evolutionary selection, a principle governing growth orientation in vapor-deposited layers, Philips Res. Rep. **22**, 267–288 (1968)

5.75 G.Z. Cao, J.J. Schermer, W.J.P. van Enckevort, W.A.L.M. Elst, L.J. Giling: Growth of {100} textured diamond films by the addition of nitrogen, J. Appl. Phys. **79**, 1357–1364 (1996)

5.76 M. Ohring: *Materials Science of Thin Films* (Academic, San Diego 2001)

5.77 D. Pan, Z. Shuyuan, Y. Chen, J.G. Hou: Hydrothermal preparation of long nanowires of vanadium oxide, J. Mater. Res. **17**, 1981–1984 (2002)

5.78 V. Petkov, P.N. Trikalitis, E.S. Bozin, S.J.L. Billinge, T. Vogt, M.G. Kanatzidis: Structure of $V_2O_5 \cdot nH_2O$ xerogel solved by the atomic pair distribution function technique, J. Am. Chem. Soc. **124**, 10157–10162 (2002)

5.79 K. Takahashi, S.J. Limmer, Y. Wang, G.Z. Cao: Synthesis, electrochemical properties of single crystal V_2O_5 nanorod arrays by template-based electrodeposition, J. Phys. Chem. B **108**, 9795–9800 (2004)

5.80 G.Z. Cao: Growth of oxide nanorod arrays through sol electrophoretic deposition, J. Phys. Chem. B **108**, 19921–19931 (2004)

5.81 R.L. Penn, J.F. Banfield: Morphology development and crystal growth in nanocrystalline aggregates under hydrothermal conditions: Insights from titania, Geochim. Cosmochim. Acta **63**, 1549–1557 (1999)

5.82 C.M. Chun, A. Navrotsky, I.A. Aksay: Aggregation growth of nanometer-sized $BaTiO_3$ particles, Proc. Microsc. Microanal. (1995) pp. 188–189

5.83 J. Livage: Synthesis of polyoxovanadates via chimie douce, Coord. Chem. Rev. **178–180**, 999–1018 (1998)

5.84 K.V. Saban, J. Thomas, P.A. Varughese, G. Varghese: Thermodynamics of crystal nucleation in an external electric field, Cryst. Res. Technol. **37**, 1188–1199 (2002)

5.85 D. Grier, E. Ben-Jacob, R. Clarke, L.M. Sander: Morphology and microstructure in electrochemical deposition of zinc, Phys. Rev. Lett. **56**, 1264–1267 (1986)

5.86 C.J. Li, Y.G. Guo, B.S. Li, C.R. Wang, L.J. Wan, C.L. Bai: Template synthesis of $Sc@C_{82}$ (I) nanowires and nanotubes at room temperature, Adv. Mater. **17**, 71–73 (2005)

5.87 Y.G. Guo, C.J. Li, L.J. Wan, D.M. Chen, C.R. Wang, C.L. Bai, Y.G. Wang: Well-defined fullerene nanowire arrays, Adv. Funct. Mater. **13**, 626–630 (2003)

5.88 B.B. Lakshmi, C.J. Patrissi, C.R. Martin: Sol-gel template synthesis of semiconductor oxide micro- and nanostructures, Chem. Mater. **9**, 2544–2550 (1997)

5.89 Q. Lu, F. Gao, S. Komarneni, T.E. Mallouk: Ordered SBA-15 nanorod arrays inside a porous alumina membrane, J. Am. Chem. Soc. **126**, 8650–8651 (2004)

5.90 J.S. Reed: *Introduction to Principles of Ceramic Processing* (Wiley, New York 1988)

5.91 C.A. Huber, T.E. Huber, M. Sadoqi, J.A. Lubin, S. Manalis, C.B. Prater: Nanowire array composite, Science **263**, 800–802 (1994)

5.92 Z. Zhang, D. Gekhtman, M.S. Dresselhaus, J.Y. Ying: Processing and characterization of single-crystalline ultrafine bismuth nanowires, Chem. Mater. **11**, 1659–1665 (1999)

5.93 E.G. Wolff, T.D. Coskren: Growth, morphology of magnesium oxide whiskers, J. Am. Ceram. Soc. **48**, 279–285 (1965)

5.94 W. Liang, C.R. Martin: Template-synthesized poly-acetylene fibrils show enhanced supermolecular order, J. Am. Chem. Soc. **112**, 9666–9668 (1990)

5.95 S.M. Marinakos, L.C. Brousseau III, A. Jones, D.L. Feldheim: Template synthesis of one-dimensional Au, Au-poly(pyrrole) and poly(pyrrole) nanoparticle arrays, Chem. Mater. **10**, 1214–1219 (1998)

5.96 H.D. Sun, Z.K. Tang, J. Chen, G. Li: Polarized Raman spectra of single-wall carbon nanotubes mono-dispersed in channels of $AlPO_4$–5 single crystals, Solid State Commun. **109**, 365–369 (1999)

5.97 Z. Cai, J. Lei, W. Liang, V. Menon, C.R. Martin: Molecular and supermolecular origins of enhanced electronic conductivity in template-synthesized polyheterocyclic fibrils. 1. Supermolecular effects, Chem. Mater. **3**, 960–967 (1991)

5.98 Y.J. Han, J.M. Kim, G.D. Stucky: Preparation of noble metal nanowires using hexagonal mesoporous silica SBA-15, Chem. Mater. **12**, 2068–2069 (2000)

5.99 J. Liu, G.E. Fryxell, M. Qian, L.-Q. Wang, Y. Wang: Interfacial chemistry in self-assembled nanoscale materials with structural ordering, Pure Appl. Chem. **72**, 269–279 (2000)

5.100 L. Chen, P.J. Klar, W. Heimbrodt, F. Brieler, M. Fröba: Towards ordered arrays of magnetic semiconductor quantum wires, Appl. Phys. Lett. **76**, 3531–3533 (2000)

5.101 T. Wen, J. Zhang, T.P. Chou, S.J. Limmer, G.Z. Cao: Template-based growth of oxide nanorod arrays by centrifugation, J. Sol-Gel Sci. Tech. **33**, 193–200 (2005)

5.102 B. Gates, Y. Wu, Y. Yin, P. Yang, Y. Xia: Single-crystalline nanowires of Ag_2Se can be synthesized by templating against nanowires of trigonal Se, J. Am. Chem. Soc. **123**, 11500–11501 (2001)

5.103 E.W. Wong, B.W. Maynor, L.D. Burns, C.M. Lieber: Growth of metal carbide nanotubes, nanorods, Chem. Mater. **8**, 2041–2046 (1996)

5.104 Y. Li, G.S. Cheng, L.D. Zhang: Fabrication of highly ordered ZnO nanowire arrays in anodic alumina membranes, J. Mater. Res. **15**, 2305–2308 (2000)

5.105 C.M. Zelenski, P.K. Dorhout: The template synthesis of monodisperse microscale nanofibers, nanotubules of MoS_2, J. Am. Chem. Soc. **120**, 734–742 (1998)

5.106 E. Braun, Y. Eichen, U. Sivan, G. Ben-Yoseph: DNA-templated assembly and electrode attachment of a conducting silver wire, Nature **391**, 775–778 (1998)

5.107 J. Zhan, X. Yang, D. Wang, S. Li, Y. Xie, Y. Xia, Y. Qian: Polymer-controlled growth of CdS nanowires, Adv. Mater. **12**, 1348–1351 (2000)

5.108 Y. Wang, K. Takahashi, H.M. Shang, G.Z. Cao: Synthesis, electrochemical properties of vanadium pentoxide nanotube arrays, J. Phys. Chem. **B109**, 3085–3088 (2005)

5.109 K. Takahashi, Y. Wang, G.Z. Cao: $Ni-V_2O_5 \cdot n\,H_2O$ core-shell nanocable arrays for enhanced electrochemical intercalation, J. Phys. Chem. B **109**, 48–51 (2005)